FULL PAPER

Dalton
www.rsc.org/dalton

Ternary iron(II) complex with an emissive imidazopyridine arm from Schiff base cyclizations and its oxidative DNA cleavage activity†

Arindam Mukherjee, Shanta Dhar, Munirathinam Nethaji and Akhil R. Chakravarty*

Department of Inorganic and Physical Chemistry, Indian Institute of Science, Bangalore, 560012, India. E-mail: arc@ipc.iisc.ernet.in; Fax: 91-80-23600683; Tel: 91-80-22932533

Received 1st October 2004, Accepted 19th November 2004
First published as an Advance Article on the web 6th December 2004

The ternary iron(II) complex $[Fe(L')(L'')](PF_6)_3$ (**1**) as a synthetic model for the bleomycins, where L′ and L″ are formed from metal-mediated cyclizations of *N*,*N*′-(2-hydroxypropane-1,3-diyl)bis(pyridine-2-aldimine) (L), is synthesized and structurally characterized by X-ray crystallography. In the six-coordinate iron(II) complex, ligands L′ and L″ show tetradentate and bidentate chelating modes of bonding. Ligand L′ is formed from an intramolecular attack of the alcoholic OH group of L to one imine moiety leading to the formation of a stereochemically constrained five-membered ring. Ligand L″ which is formed from an intermolecular reaction involving one imine moiety of L and pyridine-2-carbaldehyde has an emissive cationic imidazopyridine pendant arm. The complex binds to double-stranded DNA in the minor groove giving a K_{app} value of 4.1×10^5 M^{-1} and displays oxidative cleavage of supercoiled DNA in the presence of H_2O_2 following a hydroxyl radical pathway. The complex also shows photo-induced DNA cleavage activity on UV light exposure involving formation of singlet oxygen as the reactive species.

Introduction

Bleomycins (BLMs) are the glycopeptide antitumor antibiotics that cleave DNA in an oxidative manner.[1–3] The structure of BLMs primarily consists of three domains having different functional roles. It has a carbohydrate domain for cell permeability and for facilitating O_2 binding, a chelation unit for binding to metal, *viz*. iron, which is also the oxygen binding site, and a C-terminus bithiazole unit with DNA binding affinity and sequence selectivity (Scheme 1). The structural and functional aspects of the BLMs–DNA interactions have earlier been studied using various BLM analogs/conjugates to determine the specific roles of different domains.[4–8] In contrast, synthetic model iron complexes are rare, possibly due to the structural complexity of BLMs.[9–15]

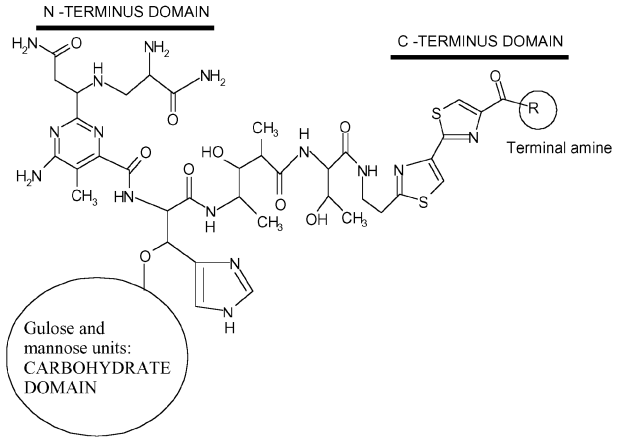

Scheme 1 Schematic structure of Bleomycins.

There are few reports on the synthetic model complexes for the metal binding site, *i.e.* the N-terminus domain.[11–14] The only iron complex with a proposed structure that models both the N- and C-terminus units was reported by Hertzberg and Dervan.[10] They have shown that methidiumpropyl-EDTA in presence of ferrous ion and oxygen under *in situ* reaction cleaves DNA in an oxidative manner. In this paper, we present the synthesis and crystal structure of a ternary iron(II) complex $[Fe(L')(L'')](PF_6)_3$ (**1**) which is formed serendipitously from novel Schiff base cyclizations involving the imine functionality of the potentially pentadentate Schiff base *N*,*N*′-(2-hydroxypropane-1,3-diyl)bis(pyridine-2-aldimine) (L) on reaction with ferric chloride in alcoholic medium in the presence of NH_4PF_6 (Scheme 2). Complex **1**, with a semi-flexible cationic aromatic DNA-binder arm that shows fluorescence, exemplifies the first structurally characterized synthetic model for the N- and C-terminus domains of BLMs. Complex **1** efficiently cleaves supercoiled plasmid DNA in the presence of H_2O_2 or UV light.

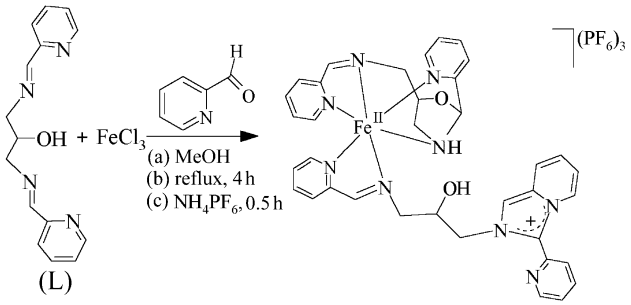

Scheme 2 Synthetic scheme for **1**. $FeCl_3$, L and pyridine-2-carbaldehyde are in 1.5, 3.75 and 1.8 mmol quantity, respectively.

Results and discussion

Synthesis and general aspects

The reaction of $FeCl_3$ with the potentially pentadentate Schiff base *N*,*N*′-(2-hydroxypropane-1,3-diyl)bis(pyridine-2-aldimine) (L) forms **1** in ~45% yield in the presence of NH_4PF_6 in an alcoholic medium. The yield is, however, significantly improved to ~70% by a modified procedure in which pyridine-2-carbaldehyde is added to the reaction mixture (Scheme 2). The crude purple product is found to contain a yellow paramagnetic impurity which is removed by column chromatography to isolate

† Electronic supplementary information (ESI) available: Fig. S1: Visible spectral traces of **1** on treatment with Ce(IV) ion followed by ascorbate; Fig. S2: Structures of the five-membered ring of L′ and the imidazopyridine ring of L″. See http://www.rsc.org/suppdata/dt/b4/b415864d/

DOI: 10.1039/b415864d

the analytically pure complex **1**. The complex is a 1 : 3 electrolyte and displays characteristic PF_6 stretching bands in the IR spectrum. It shows electronic spectral d–d bands at 516 and 592 nm and an emission band at 392 nm (317 nm excitation) in MeCN (Fig. 1). The complex is also emissive at 389 nm (315 nm excitation) in an aqueous medium. The emission intensity is found to increase slowly with time. After *ca.* 30 min, it reaches its maximum. It is likely that the complex is susceptible to hydrolysis in the aqueous medium at the metal-bound imine bond of L″ causing the imidazopyridine arm to slowly dissociate from the complex over a period of time.

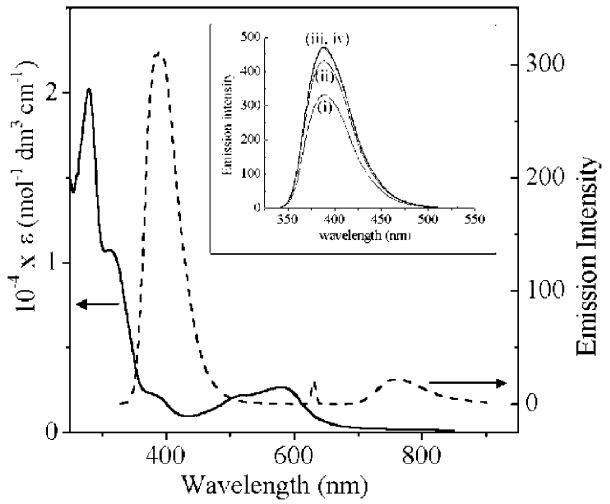

Fig. 1 UV-vis (—) and emission (---, 317 nm excitation) spectra of **1** in MeCN. The inset shows the emission spectra of the complex in aqueous medium at different time intervals [t = 0 min (i); 10 min (ii); 20 min (iii); 30 min (iv)].

The complex is redox active and displays a quasi-reversible cyclic voltammetric response assignable to the Fe(III)/Fe(II) couple at 0.98 V *vs.* SCE (ΔE_p, ~90 mV at 50–500 mV s^{-1}) in MeCN–0.1 M TBAP (Fig. 2).[16] It undergoes chemical oxidation on addition of Ce(IV) ion with a reduction of the intensity of the purple band to a colorless solution which regenerates **1** on reaction with sodium ascorbate in aqueous MeCN solvent (Fig. S1. ESI†).

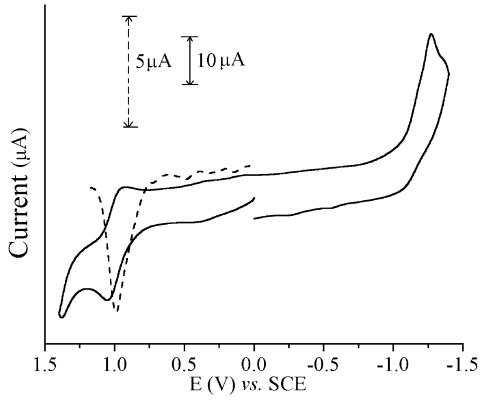

Fig. 2 The cyclic voltammogram (—) and differential pulse voltammogram (---) of **1** showing the Fe(III)/Fe(II) redox couple in MeCN–0.1 M TBAP at 50 mV s^{-1} for CV and 5 mV s^{-1} for DPV (pulse height = 25 mV, drop time = 0.4 s).

Crystal structure

Complex **1** has been structurally characterized by X-ray crystallography. The structure shows the presence of the cationic iron(II) complex and three PF_6 anions in the crystallographic asymmetric unit (Fig. 3).[17] Selected bond distances and angles are given in Table 1. In the ternary structure, L′ and L″ display tetradentate and bidentate modes of binding, respectively, in an essentially octahedral $Fe^{II}N_6$ coordination geometry. The av. Fe–N bond length is ~2.0 Å with the Fe(1)–N(3) bond length (2.036(6) Å) being significantly longer than the rest. Both L′ and L″ are formed from the Schiff base L by metal-promoted Schiff-base cyclization reactions. Ligand L′ is formed from an intramolecular attack of the alcoholic OH group to one imine bond of L resulting in a stereochemically constrained five-membered ring that is expected to make the relatively long Fe(1)–N(3) bond vulnerable to substitution in the DNA cleavage reactions (Fig. S2a, ESI†). The mono-cationic L″ is presumably formed from an intermolecular reaction involving one imine moiety of L with pyridine-2-carbaldehyde present in the reaction mixture.

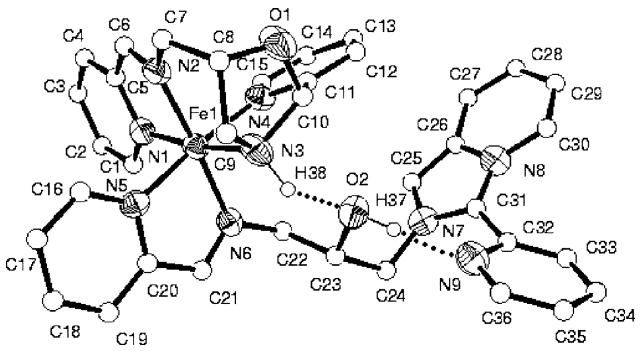

Fig. 3 A perspective view of the cationic complex in $[Fe(L')(L'')](PF_6)_3$ (**1**) showing the pendant arm and the hydrogen bonding interactions.

Ligand L″ has a long pendant arm whose flexibility is significantly reduced in the presence of hydrogen bonding interactions involving the N(3)H(38) group of L′, the O(2)H(37) group and the non-coordinated pyridine nitrogen atom N(9) of L″ [N(3)···O(2), 2.890(9) Å; O(2)···N(9), 2.838(9) Å]. Atoms H(37) and H(38) were located from the difference Fourier maps and refined isotropically. The fused five- and six-membered rings in the imidazo[1,5-*a*]pyridine moiety of L″ are essentially coplanar (dihedral angle: ~1.0°) (Fig. S2b, ESI†). The bond distances in this unit lie in the range of 1.348(11) to 1.439(10) Å giving an av. distance of 1.38 Å which is similar to the C–C bond distances observed in the pyridyl rings (Table 2). Both the N(7) and N(8) atoms are planar showing a sum of three angles as 360°. This unit is mono-cationic and aromatic with the positive charge being delocalized on N(7) or N(8), giving a resonance structure (Scheme 2). There are four double bonds in this unit. Contribution of 2e$^-$ from the nitrogen atom makes 10π-electrons in total needed for aromaticity.

DNA cleavage studies

The binding of **1** to calf thymus (CT) DNA has been studied by fluorescence spectral method using the emission intensity of ethidium bromide (EB). EB does not show any emission

Table 1 Selected bond distances (Å) and bond angles (°) data for $[Fe(L')(L'')](PF_6)_3$ (**1**)

Fe(1)–N(1)	1.990(6)	Fe(1)–N(4)	2.007(5)
Fe(1)–N(2)	1.975(6)	Fe(1)–N(5)	1.991(5)
Fe(1)–N(3)	2.036(6)	Fe(1)–N(6)	1.995(5)
N(2)–Fe(1)–N(1)	81.2(3)	N(5)–Fe(1)–N(4)	174.4(2)
N(2)–Fe(1)–N(5)	95.9(2)	N(6)–Fe(1)–N(4)	93.2(2)
N(1)–Fe(1)–N(5)	89.7(2)	N(2)–Fe(1)–N(3)	91.5(3)
N(2)–Fe(1)–N(6)	176.9(2)	N(1)–Fe(1)–N(3)	171.4(2)
N(1)–Fe(1)–N(6)	97.8(2)	N(5)–Fe(1)–N(3)	95.5(2)
N(5)–Fe(1)–N(6)	81.2(2)	N(6)–Fe(1)–N(3)	89.8(2)
N(2)–Fe(1)–N(4)	89.7(2)	N(4)–Fe(1)–N(3)	83.5(2)
N(1)–Fe(1)–N(4)	92.0(2)		

Table 2 Selected bond distances (Å) for the cyclized moieties of $[Fe(L')(L'')](PF_6)_3$ (**1**)

Five-membered ring in L′			
O(1)–C(8)	1.465(9)	C(7)–C(8)	1.492(11)
O(1)–C(10)	1.434(8)	C(8)–C(9)	1.520(11)
N(3)–C(9)	1.502(9)	C(10)–C(11)	1.489(10)
N(3)–C(10)	1.527(8)		
Imidazopyridine moiety in L″			
N(7)–C(25)	1.363(8)	C(27)–C(28)	1.371(12)
N(7)–C(31)	1.370(8)	C(28)–C(29)	1.405(12)
N(8)–C(26)	1.408(9)	C(29)–C(30)	1.348(11)
N(8)–C(30)	1.416(9)	C(31)–C(32)	1.479(9)
N(8)–C(31)	1.359(8)	C(32)–C(33)	1.375(10)
N(9)–C(32)	1.364(9)	C(33)–C(34)	1.381(11)
N(9)–C(36)	1.334(11)	C(34)–C(35)	1.382(12)
C(25)–C(26)	1.368(10)	C(35)–C(36)	1.382(11)
C(26)–C(27)	1.439(10)		

in the buffer medium due to fluorescence quenching by the solvent molecules.[18] In the presence of CT DNA, it shows emission due to its intercalative binding to DNA. Addition of **1** with its cationic planar imidazopyridine moiety results in the competitive binding to DNA causing reduction of the emission intensity due to displacement of the EB from the bound to the free state (Fig. 4). The apparent binding constant (K_{app}) is estimated as 4.1×10^5 M^{-1} [K_{app} (EB) = 10^7 M^{-1}].[19] The emission spectral behavior of complex **1** in the presence of CT DNA has been studied. The emission intensity is found to increase with time until it reaches a constant value after *ca.* 30 min (Fig. 4).

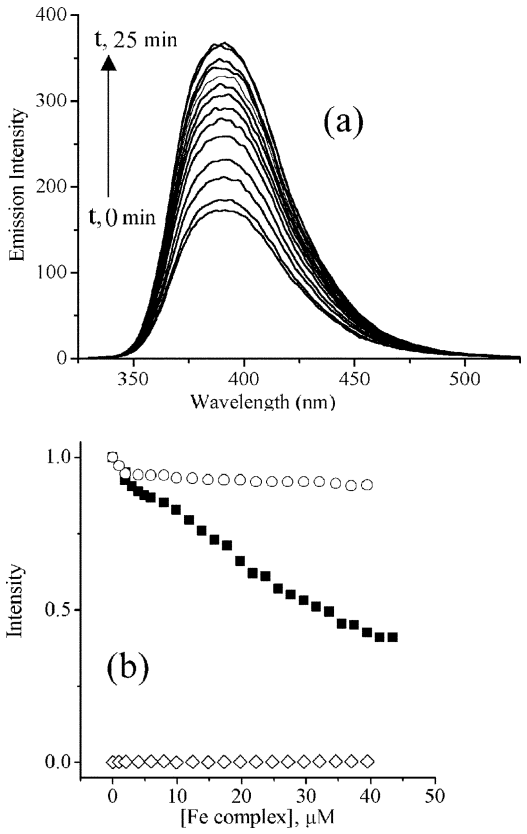

Fig. 4 (a) Emission spectral traces of $[Fe(L')(L'')](PF_6)_3$ (**1**, 5 μM) showing enhancement of intensity at 390 nm (excitation wavelength: 317 nm) with time in the presence of CT DNA (303 μM) in Tris-HCl/NaCl buffer (50 mM, pH 7.2). (b) The effect of addition of **1** (■) and Na[Fe(EDTA)] (○) to the emission intensity of 303 μM calf thymus DNA-bound ethidium bromide (1.3 μM) in a 5 mM Tris-HCl buffer (pH, 7.2) at 25 °C (◇, the emission intensities of the ethidium bromide in the absence of CT DNA but at different concentrations of **1**).

The observation which is similar to that evidenced in the absence of DNA, suggests cleavage of the imidazopyridine arm from the complex. The results indicate significant quenching effect of the $\{FeL'\}^{2+}$ unit even in the absence of any π-conjugation between the metal-bound imine moiety and the imidazopyridine group of L″.

The oxidative DNA cleavage activity of the complex was studied in the presence of H_2O_2 or on photo irradiation. The complex is cleavage inactive in the presence of reducing agents, but cleaves supercoiled (SC) pUC19 DNA when treated with H_2O_2 or on exposure to UV light (Figs. 5 and 6). Selected DNA cleavage data are given in Table 3. Control experiments show that H_2O_2 or **1** alone, under aerobic conditions, is cleavage inactive in dark. A 30 μM solution of **1** cleaves SC DNA (~500 ng) to the extent of ~93% on treatment with 53 μM H_2O_2. A significant cleavage of DNA is also observed at 10 μM complex solution using 88 μM H_2O_2. Control experiments also reveal the minor groove binding of **1** as addition of distamycin completely inhibits the cleavage. A similar inhibition is observed in the presence of DMSO suggesting the possibility of the formation of $^{\bullet}OH$ radicals as the reactive species from probable hydroperoxo intermediate: $[Fe^{III}–OOH^-]^{2+} \rightarrow [Fe^{IV}=O]^{2+} + {}^{\bullet}OH$.[20] DNA cleavage efficiency of **1** is significantly more than Na[Fe(EDTA)] which shows only ~26% cleavage, while **1** cleaves ~75% using 25 μM complex and 53 μM H_2O_2.

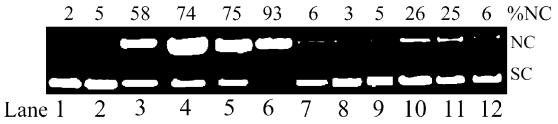

Fig. 5 Gel electrophoresis diagram showing the cleavage of SC pUC19 DNA (0.5 μg) by **1** in Tris-HCl/NaCl buffer (pH 7.2) in dark for 45 min reaction time: Lane 1, DNA control; lane 2, DNA + H_2O_2 (88 μM); lane 3, DNA + **1** (10 μM) + H_2O_2 (70 μM); lane 4, DNA + **1** (10 μM) + H_2O_2 (88 μM); lane 5, DNA + **1** (25 μM) + H_2O_2 (53 μM); lane 6, DNA + **1** (30 μM) + H_2O_2 (53 μM); lane 7, DNA + distamycin (100 μM) + **1** (25 μM) + H_2O_2 (53 μM); lane 8, DNA + DMSO (4 μL) + **1** (25 μM) + H_2O_2 (53 μM); lane 9, DNA + $FeCl_3$ (25 μM) + H_2O_2 (53 μM); lane 10, DNA + Na[Fe(EDTA)] (25 μM) + H_2O_2 (53 μM); lane 11, DNA + **1** (50 μM) + dithiothreitol (DTT, 5 mM); lane 12, DNA + **1** (50 μM) + 3-mercaptopropionic acid (MPA, 5 mM).

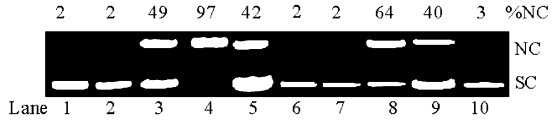

Fig. 6 Photocleavage of SC DNA (0.5 μg) by **1**. Lanes 1–9 in air and lane 10 under argon. Lane 1, DNA control (λ = 312 nm); lane 2, DNA + **1** (in dark); lane 3, DNA + **1** (50 μM, 312 nm, 5 min); lane 4, DNA + **1** (50 μM, 312 nm, 10 min); lane 5, DNA + **1** (50 μM); lane 6, DNA + NaN_3 (100 μM) + **1**; lane 7, DNA + L-histidine (100 μM) + **1**; lane 8, DNA + D_2O (14 μL) + **1**; lane 9, DNA + DMSO (4 μL) + **1**; lane 10, DNA + **1** (under argon) [lanes 5–10: **1** (50 μM, 365 nm, 10 min)].

The light-induced DNA cleavage has been studied at 312 and 365 nm. A 50 μM **1** at 312 nm cleaves ~97% of DNA (~500 ng) for an exposure of 10 min. The extent of cleavage at 365 nm is ~42% on 10 min photoexposure. Further investigations reveal an enhancement of cleavage in D_2O, complete inhibition in the presence of azide or L-histidine, and no apparent inhibition in DMSO. Complete inhibition is observed under argon. The results are indicative of the formation of singlet oxygen ($^1O_2$) as the reactive species in a type-II process by involving the cationic imidazopyridine moiety of L″ as a photosensitizer: (i) $[Fe^{II}(L')(L'')]^{3+}$ (I) + hν → $[Fe^{II}(L')(L'')^*]^{3+}$ (I*); (ii) I* + $^3O_2$ → I + $^1O_2$.[21]

Table 3 Selected cleavage data[a] of SC pUC19 (500 ng) DNA by **1** on chemical oxidation and photo-irradiation

No	Reaction condition	[**1**]/μM	[H_2O_2]/μM	λ/nm	t^b/min	DNA cleavage (%)
Chemical nuclease data						
1	DNA control	—	—	—	—	2
2	DNA + H_2O_2	—	88	—	—	5
3	DNA + **1** + H_2O_2	10	88	—	—	74
4	DNA + **1** + H_2O_2	30	53	—	—	93
5	DNA + **1** + DMSO[c] + H_2O_2	25	53	—	—	3
6	DNA + distamycin[d] + **1** + H_2O_2	25	53	—	—	6
Photocleavage data						
7	DNA control	—	—	312	10	2
8	DNA + **1**	50	—	Dark	10	2
9	DNA + **1**	50	—	312	10	97
10	DNA + **1**	50	—	365	10	42
11	DNA + **1** + NaN_3[e]	50	—	365	10	2
12	DNA + **1** + DMSO[c]	50	—	365	10	40

[a] Incubation time 45 min in dark. [b] *t*, exposure time. [c] 4 μL. [d] 100 μM. [e] 100 μM.

Conclusion

The ternary complex **1** is the first structurally characterized iron(II) complex modeling the N- and C-terminus domains of bleomycins. The ligands L′ and L″ are formed from novel metal-mediated Schiff base cyclizations of the Schiff base L. The DNA cleavage reaction of **1** involves the cationic arm as a minor groove binder and the redox active iron center to form the reactive hydroxyl species. Ligand L″ with an emissive cationic pendant aromatic imidazopyridine ring acts as a photosensitizer. Isolation of **1** is of significance as imidazopyridines are known to be potential antitumor antibiotics.[22–24]

Experimental

All reagents and chemicals were purchased from commercial sources and used without further purifications except MeCN, which was purified by standard procedures before use in electrochemical measurements.[25] The Schiff base ligand *N*,*N*′-(2-hydroxypropane-1,3-diyl)bis(pyridine-2-aldimine) (L) was prepared by a reported method.[26] The elemental analysis was done using Thermo Finnigan FLASH EA 1112 CHN analyser instrument. The IR and electronic spectral measurements were done using Perkin-Elmer Spectrum One FT-IR and Lambda 55 spectrometers, respectively. Cyclic and differential pulse voltammetric measurements were made at 25 °C on a EG&G PAR 253 VersaStat potentiostat/galvanostat using a three-electrode configuration consisting of a glassy carbon working, a platinum wire auxiliary and a saturated calomel reference (SCE) electrode. Ferrocene ($E_{\frac{1}{2}}$ = 0.41 V) was used as a standard in MeCN–0.1 M [Bu^n_4N]ClO_4 (TBAP). Conductivity measurements were made at 25 °C using a Control Dynamics conductivity meter.

Preparation of [Fe(L′)(L″)](PF$_6$)$_3$ (1)

A 10 ml methanolic solution of $FeCl_3$ (0.243 g, 1.5 mmol) was added slowly to a magnetically stirred 15 ml methanolic solution of the ligand L (1.0 g, 3.75 mmol). The solution was then refluxed under stirring for 15 min and pyridine-2-carbaldehyde (0.17 ml, 1.8 mmol) was added. The mixture was refluxed for 4 h. A 5 ml methanolic solution of NH_4PF_6 (1.16 g, 7.14 mmol) was then added to the reaction mixture and solution was heated for a further period of 30 min. The solution was cooled to an ambient temperature. A purple solid was precipitated on slow concentration of the solution. The solid was isolated, washed with ethanol and dried in *vacuo* (yield: 1.17 g, ~70%). The complex in an analytically pure form was isolated by column chromatography using neutral alumina column (45 cm length, 1.5 cm diameter) by loading 0.18 g of the crude product and elution was done using an MeCN–MeOH mixture (7 : 3 v/v) under nitrogen atmosphere. A minor yellow fraction as an impurity was eluted first. The major purple band containing complex **1** was eluted next. The complex was isolated in essentially quantitative yield after removal of the solvent. Anal. Calc. for $C_{36}H_{36}F_{18}FeN_9O_2P_3$: C, 38.9; H, 3.5; N, 11.6. Found: C, 38.7; H, 3.3; N, 11.3%. FT-IR (KBr phase), cm^{-1}: 3643br, 3418br, 3118br, 1613m, 1550w, 1470m, 1444w, 1294m, 1275w, 1253w, 1162w, 1115w, 1075w, 984m, 840vs (PF_6), 771s, 558s, 519w (br, broad; w, weak; m, medium; s, strong; vs, very strong). UV-vis in MeCN [λ_{max}/nm (ε/mol^{-1} dm^3 cm^{-1})]: 282 (19500), 321 (11300), 379 (5000), 516 (4600), 592 (6700). Conductance in MeCN [Λ_M/Ω^{-1} cm^2 mol^{-1}]: 415.

X-Ray crystallography

Crystal data for $C_{36}H_{36}F_{18}FeN_9O_2P_3$, M = 1117.5, triclinic, space group $P\bar{1}$ (no. 2), a = 9.449(5), b = 15.793(8), c = 17.694(9) Å, α = 108.047(8), β = 102.452(9), γ = 107.097(8)°, U = 2259(2) Å^3, Z = 2, T = 293(2) K, D_c = 1.643 g cm^{-3}, $R1$ = 0.0929, $wR2$ = 0.2076 for 4105 reflections with $I > 2\sigma(I)$ and 630 parameters [$R1$ (F^2) = 0.1856 (all data)]. Weighting scheme: $w = 1/[\sigma^2(F_o^2) + (0.1278P)^2 + 2.4628P]$, where $P = [F_o^2 + 2F_c^2]/3$. X-Ray data from a Bruker SMART APEX CCD diffractometer. The structure was solved and refined by SHELX programs.[27]

Single crystals of complex **1** were obtained by vapour diffusion of diethyl ether into an acetonitrile solution of the complex. A prismatic single crystal was mounted on a glass fiber with epoxy cement. All the X-ray diffraction data were measured in frames with increasing ω (width of 0.3° $frame^{-1}$) and with a scan speed at 15 s $frame^{-1}$ on a Bruker SMART APEX CCD diffractometer, equipped with a fine focus 1.75 kW sealed tube X-ray source. Empirical absorption corrections were carried out using a multi-scan program.[28] The structure was solved by the heavy atom method and refined by full-matrix least squares using the SHELX system of programs.[27] All non-hydrogen atoms were refined anisotropically. The hydrogen atoms attached to carbon atoms in **1** were generated and assigned isotropic thermal parameters, riding on their parent carbon atoms, and used for structure factor calculation only. The hydrogen atoms of the –OH and −NH groups were located from the difference Fourier maps and they were refined two cycles isotropically at the initial stage. At the final stage of refinement, their thermal parameters were only refined isotropically. The goodness-of-fit was 0.89. The maximum shift/e.s.d. was 0.004.

CCDC reference number 240419.

See http://www.rsc.org/suppdata/dt/b4/b415864d/ for crystallographic data in CIF or other electronic format.

DNA-binding and cleavage experiments

The concentration of the calf thymus DNA (125 μM) was determined from its absorption intensity at 260 nm with a known ε value of 6600 $dm^3\ mol^{-1}\ cm^{-1}$.[29] The binding of complex **1** to calf thymus (CT) DNA was studied by fluorescence spectral method using the emission intensity of ethidium bromide (EB). The apparent binding constant (K_{app}) value for **1** was estimated from the equation: $K_{EB}[EB] = K_{app}[complex]$ using the K_{app} value of EB as $10^7\ M^{-1}$.[19]

The DNA cleavage activity of the complex was studied by agarose gel electrophoresis. Supercoiled pUC19 DNA (6 μl, ~500 ng) in Tris-HCl buffer (50 mM, pH 7.2) containing NaCl (50 mM) was treated with the complex in the presence or absence of additives. The oxidative DNA cleavage by the complex (10–30 μM) was studied in the presence of hydrogen peroxide of different concentrations varying from 53 to 88 μM. The sample was incubated first for 1 h at 37 °C and then added loading buffer (25% bromophenol blue, 0.25% xylene cyanol, 30% glycerol (3 μl)) and finally loaded on 0.8% agarose gel containing 1.0 μg ml^{-1} EB. Electrophoresis was carried out at 40 V for 2.0 h in Tris-acetate EDTA (TAE) buffer. Bands were visualized by UV light and photographed. The cleavage activity was measured by determining the ability of the complex in relaxing the SC DNA to its nicked circular (NC) form. The proportion of DNA in the SC and NC form after electrophoresis was estimated quantitatively from the intensities of the bands using a UVITEC Gel Documentation System with due correction of the low level of NC present in the original sample and the low affinity of EB binding to SC compared to NC and linear forms of DNA.[30] The photo-induced pUC19 DNA cleavage studies were carried out using monochromatic UV lights of 312 nm (96 W total wattage) and 365 nm (12 W). Control experiments were done using different reagents such as sodium azide (100 μM), DMSO (4 μL), D_2O (14 μL), L-histidine (100 μM), distamycin (100 μM) added to SC DNA prior to the addition of the complex.

Acknowledgements

We thank the Department of Science and Technology, Government of India, for funding and the diffractometer facility, the Council of Scientific and Industrial Research, New Delhi, for funding, and the Alexander von Humboldt Foundation, Germany, for donation of an electroanalytical system.

References

1 H. Umezawa, *Prog. Biochem. Pharmacol.*, 1976, **11**, 18.
2 R. M. Burger, *Chem. Rev.*, 1998, **98**, 1153.
3 S. E. Wolkenberg and D. L. Boger, *Chem. Rev.*, 2002, **102**, 2477.
4 D. L. Boger and H. Cai, *Angew. Chem., Int. Ed.*, 1999, **38**, 448.
5 M. Otsuka, T. Masuda, A. Haupt, M. Ohno, T. Shiraki, Y. Sugiura and K. Maeda, *J. Am. Chem. Soc.*, 1990, **112**, 838.
6 C. J. Thomas, M. M. McCormick, C. Vialas, Z.-F. Tao, C. J. Leitheiser, M. J. Rishel, X. Wu and S. M. Hecht, *J. Am. Chem. Soc.*, 2002, **124**, 3875.
7 A. K. Choudhury, Z.-F. Tao and S. M. Hecht, *Org. Lett.*, 2001, **3**, 1291.
8 M. J. Rishel, C. J. Thomas, Z.-F. Tao, C. Vialas, C. J. Leitheiser and S. M. Hecht, *J. Am. Chem. Soc.*, 2003, **125**, 10194.
9 G. Pratviel, J. Bernadou and B. Meunier, *Adv. Inorg. Chem.*, 1998, **45**, 251.
10 R. P. Hertzberg and P. B. Dervan, *J. Am. Chem. Soc.*, 1982, **104**, 313.
11 R. J. Guajardo, F. Chavez, E. T. Farinas and P. K. Mascharak, *J. Am. Chem. Soc.*, 1995, **117**, 3883.
12 C. Nguyen, R. J. Guajardo and P. K. Mascharak, *Inorg. Chem.*, 1996, **35**, 6273.
13 D. Y. Dawson, S. E. Hudson and P. K. Mascharak, *J. Inorg. Biochem.*, 1992, **47**, 109.
14 I. Lippai, R. S. Magliozzo and J. Peisach, *J. Am. Chem. Soc.*, 1999, **121**, 780.
15 H. Kurosaki, Y. Ishikawa, K. Hayashi, M. Sumi, Y. Tanaka, M. Goto, K. Inada, I. Taniguchi, M. Shionoya, H. Matsuo, M. Sugiyama and E. Kimura, *Inorg. Chim. Acta*, 1999, **294**, 56.
16 X. Tao, D. W. Stephan and P. K. Mascharak, *Inorg. Chem.*, 1987, **26**, 754; P. George, G. I. H. Hanania and D. H. Irvin, *J. Chem. Soc.*, 1959, **26**, 2548.
17 M. N. Brunett and C. K. Johnson, *ORTEP-III, Report ORNL-6895*, Oak Ridge National Laboratory, Oak Ridge, TN, 1996..
18 M. J. Waring, *J. Mol. Biol.*, 1965, **13**, 269.
19 M. Lee, A. L. Rhodes, M. D. Wyatt, S. Forror and J. A. Hartley, *Biochemistry*, 1993, **32**, 4237.
20 J.-U. Rohde, J.-H. In, M. H. Lim, W. W. Brennessel, M. R. Bukouski, A. Stubna, E. Münck, W. Nam and L. Que Jr., *Science*, 2003, **299**, 1037.
21 J. C. Quada, M. J. Levy and S. M. Hecht, *J. Am. Chem. Soc.*, 1993, **115**, 12171.
22 C. J. Dinsmore, C. B. Zartman, W. F. Baginsky, T. J. O'Neill, K. S. Koblan, I.-W. Chen, D. A. McLoughlin, T. V. Olah and J. R. Huff, *Org. Lett.*, 2000, **2**, 3473.
23 Z. Wu, M. E. Fraley, M. T. Bilodeau, M. L. Kaufman, E. S. Tasber, A. E. Balitza, G. D. Hartman, K. E. Coll, K. Rickert, J. Shipman, B. Shi, L. Sepp-Lorenzino and K. A. Thomas, *Bioorg. Med. Chem. Lett.*, 2004, **14**, 909.
24 M. P. Singh, S. Sasmal, W. Lu and M. N. Chatterjee, *Synthesis*, 2000, 1380; C. Hemmert, M. Renz, H. Gornitzka, S. Soulet and B. Meunier, *Chem. Eur. J.*, 1999, **5**, 1766.
25 D. D. Perrin, W. L. F. Amarego and D. R. Perrin, *Purification of Laboratory Chemicals*, Pergamon, Oxford, 2nd edn., 1980.
26 W. Mazurek, K. J. Berry, K. S. Murray, M. J. O'Connor, M. R. Snow and A. G. Wedd, *Inorg. Chem.*, 1982, **21**, 3071.
27 G. M. Sheldrick, *SHELX-97, A Computer Program for Crystal Structure Solution and Refinement*, Universität Göttingen, Göttingen, Germany, 1997.
28 G. M. Sheldrick, *SADABS, Version 2. Multi-Scan Absorption Correction Program*, Universität Göttingen, Göttingen, Germany, 2001.
29 M. E. Reichman, S. A. Rice, C. A. Thomas and P. Doty, *J. Am. Chem. Soc.*, 1954, **76**, 3047.
30 J. Bernadou, G. Pratviel, F. Bennis, M. Girardet and B. Meunier, *Biochemistry*, 1989, **28**, 7268.